ELSEVIER

Chemical Engineering Journal 72 (1999) 229–233

Chemical Engineering Journal

Kinetic study of leaching process of Raney silver catalyst

Sleem ur Rahman*, M.A. Al-Saleh

Department of Chemical Engineering, King Fahd University of Petroleum and Minerals, Dhahran 31261, Saudi Arabia

Received 8 May 1998; received in revised form 15 November 1998; accepted 24 November 1998

Abstract

Kinetic data are obtained for the leaching of Raney Ag–Al alloy (50 wt% Ag) at constant temperature and constant alkali concentration in the temperature range of 283–313 K for different average particle size. The data fit well into a developed model based on autocatalytic reactions, $\log(y/(1-y))=-a/t+ab$, where y is the fractional leaching, t is the reaction time and a and b are rate parameters. © 1999 Elsevier Science S.A. All rights reserved.

Keywords: Leaching; Kinetics; Raney Ag catalyst; Modeling

1. Introduction

Raney-silver is an effective catalyst for cathodic oxygen reduction. It is used in making gas diffusion electrodes for fuel-cells and batteries [1,2]. The silver catalyst is prepared from an aluminum–silver alloy. The finely powdered alloy is treated with hot alkali solution. Aluminum is leached out, leaving behind an active porous catalyst. The reaction products are hydrogen and sodium aluminate [3]:

$$Al + 3NaOH \rightarrow Na_3AlO_3 + 3/2\,H_2 \uparrow$$

Kinetics of the leaching process depends on a number of physicochemical processes which are affected by various parameters, e.g., particle size, alkali concentration, stirring speed, temperature, solid-to-liquid ratio etc., rendering exact theoretical analysis difficult. Experimental kinetic study of leaching of Raney Ni–Al alloy was done by Chaudhari [4] and Choudhary et al. [5]. Nevertheless similar study on Raney Ag–Al alloy is non-existent. Present work is undertaken to investigate the kinetics of Raney Ag–Al alloy. Extent of reaction at any given time can be determined either by monitoring aluminate concentration or by measuring produced hydrogen gas. As observed by Chaudhari [4], kinetic analysis of Raney alloy by following produced hydrogen is difficult and may be erroneous. In the present work rate data were obtained by determining leached aluminum. A mathematical model based on auto-catalytic reactions is also developed.

*Corresponding author. Fax: +966-3-860-4234; e-mail: srahman@kfupm.edu.sa

2. Experiments and data analysis

Leaching of Raney silver alloy was carried out in a special stirred glass reactor and sampling device. The reactor was a glass vessel of 2000 ml capacity having openings for stirrer, thermometer and sampling tube. A glass stopper at the top was fixed for the introduction of the alloy powder. For sampling out the leached solution, a tube with a fritted glass end was dipped into the reaction solution. This tube was connected to an air-tight sampler which was further connected to a three-way valve allowing introduction of pressurized air or vacuum whenever desired. The experimental set-up is shown in Fig. 1. The sample was withdrawn by applying vacuum. Pressurized air ensured quick return of excess solution to minimize sampling error.

Raney-Ag alloy powder having composition of 50% Ag and 50% Al was sieved to get narrow particle size cuts. Three different average particle sizes, 50, 95 and 185 μm were chosen, to register the effect of particle size on the leaching process. A known mass of a particular particle size was leached at a predetermined temperature with NaOH solution of 6.25 mmol cm^{-3} concentration. This concentration was selected on the basis of common practice in the leaching of Raney-Alloy [3]. The alkali solution was heated to desired temperature and hydrogen gas bubbled to saturate the solution and to remove the dissolved oxygen. After the introduction of alloy, the samples were taken out at regular time intervals. Mass of the alloy, sample volume and reactant volume were chosen such as to minimize sampling error. About 2.0 gm alloy was added to 1000 ml of alkali solution while the volume of the sample was 5 ml. Due to the small

1385-8947/99/$ – see front matter
PII: S1385-8947(99)00008-X

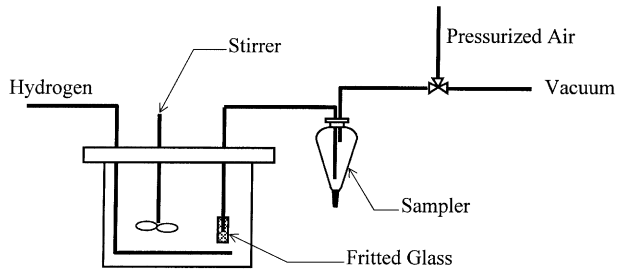

Fig. 1. Experimental set-up for the leaching of Raney-Ag alloy.

Table 1
Leaching parameters

Composition of alloy	50% Ag+50% Al
Concentration of NaOH	6.25 mmol cm^{-3}
Temperature	283–313 K
Particle size	50, 95 and 185 μm
Stirring speed	1500 rpm

amount of the sample, no significant increase in the temperature was observed, although the reaction is exothermic. The alkali concentration also did not change considerably due to the same reason. In order to eliminate any external mass-transfer resistance, the particle must be in suspension. The critical stirring speed to achieve complete suspension was estimated about 500 rpm for our system [6]. The stirring speed of 1500 rpm in these experiments ensured complete suspension of particles. All the leaching parameters for leaching are listed in Table 1.

Samples obtained from leaching experiments were analyzed for aluminum concentration by EDTA back titration using ASTM test method [7]. The fractional leaching was calculated using the following equation:

$$y = \frac{\text{amount of Al dissolved}}{\text{total amount of Al present in the alloy}}. \quad (1)$$

The fractional leaching is plotted in Fig. 2 against time for temperature 283, 288, 298 and 313 K for 95 μm particle size. Similar curves are plotted in Fig. 3 for 50, 95 and 185 μm particle size keeping the temperature constant. It is evident that the rate of the reaction is faster in the beginning and it gets slower as the reaction progresses. Instantaneous fractional leaching is higher at higher temperature and smaller particle size when compared, respectively, for same particle size and at the same temperature.

3. Kinetic modeling

The starting alloy particles are non-porous solid, but as leaching progresses aluminum is removed leaving behind a porous structure. With the assumptions of spherical particles and homogeneous aluminum distribution, the process corresponds to the shrinking core model proposed by Levenspiel [8]. The kinetic data obtained in this investigation failed to fit in the shrinking core model (i.e. plots of $1-(1-y)^{1/3}$ vs. time were not linear) suggesting more complex phenomena.

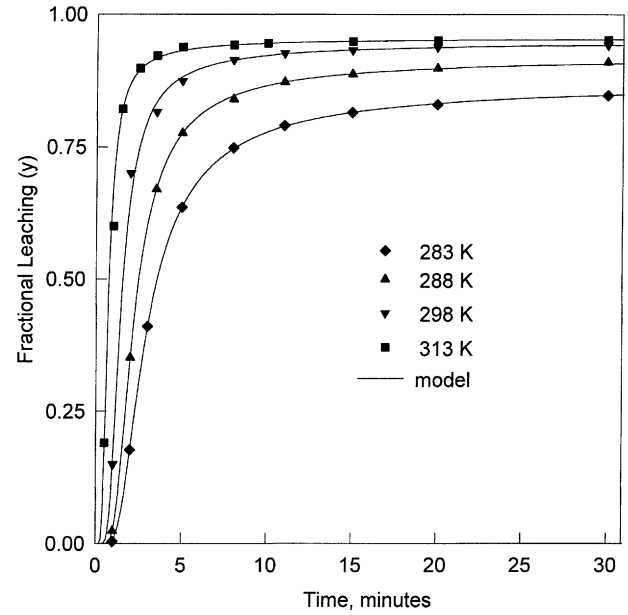

Fig. 2. Fractional leaching vs. time curves at different temperatures for average particle size of 95 μm.

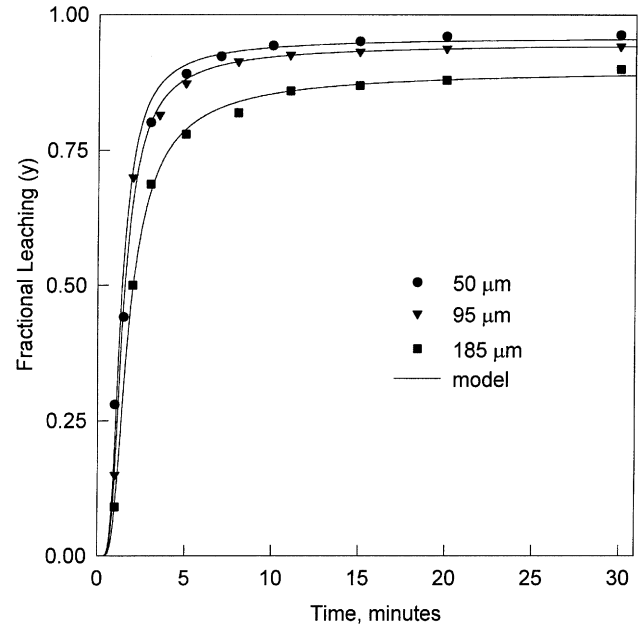

Fig. 3. Fractional leaching vs. time curves for different average particle size at 298 K.

At room temperature, a 50% Ag and 50% Al alloy has two distinct phases, namely; pure aluminum and an aluminum-rich peritectodial ξ-phase (cf. Ag–Al binary phase diagram in Ref. [9]). As the leaching progresses, aluminum concentration in the alloy decreases and recrystallization occurs resulting into formation of μ-phase (Ag_3Al). Subsequent

aluminum dissolution will increase silver concentration and eventually result into removal of all aluminum. It can be inferred that the leaching involves phase transformation from a mixture of Al and ξ-phases, via μ-phase, to Ag. At any given state of leaching, one or more phases may be present but concentration of Al-rich phases decrease with reaction progress. Since the solubilities of aluminum-rich phases are higher, leaching slows down with time. In addition, selective dissolution of aluminum and subsequent recrystallization give rise to fine cracks. Presence of porous structure further affects leaching adversely as pore diffusion will become significant. This mechanism is similar to autocatalytic reaction in solids involving nucleation, chain branching and termination steps. Prout and Tompkins [10] equation describes the kinetics of autocatalytic reactions as follows:

$$\frac{dy}{dt} = k[y(1-y)]. \tag{2}$$

Apparently due to phase change of Ag–Al alloy at various compositions, the rate constant k is time dependent. It can be assumed to vary inversely with time as done by Gregg et al. [11] for sintering of solids and Choudhary et al. [5] for leaching of Al–Ni alloy. But present data do not fit into this model. Keeping in view the sharp changes in rates, k is assumed to be inversely proportional to the square of time. Therefore Eq. (2) can be written as

$$\frac{dy}{dt} = \frac{a}{t^2}[y(1-y)]. \tag{3}$$

Integrating this equation one gets:

$$\log\left[\frac{y}{(1-y)}\right] = -\frac{a}{t} + c. \tag{4}$$

The integration constant can be obtained by introducing a parameter called half-life ($t_{1/2}$), defined as the time in which half of the original amount of the aluminum is leached. Thus, substitution of y=0.5 at t=$t_{1/2}$ results into:

$$c = a/t_{1/2} = ab, \tag{5}$$

where b=1/$t_{1/2}$.

Substitution of c in Eq. (4) gives the final form of the model equation:

$$\ln\left[\frac{y}{(1-y)}\right] = -\frac{a}{t} + ab. \tag{6}$$

4. Result and discussion

Experimental data obtained at various temperatures and for different particle size are plotted as ln[y/(1−y)] vs. 1/t in Figs. 4 and 5 which exhibit agreement with Eq. (6) (R^2>96%). The half-life periods, $t_{1/2}$, were estimated from experimental curves and compared with model prediction ($t_{1/2}$=1/b) in Table 2. Estimated half-life periods are close to the experimental values. Estimates of intercepts and slopes of fitted curves give values of $a\times b$ and $-b$ from which parameters a and b were calculated as in Table 2. Plots of these parameters against inverse of temperature in Fig. 6 indicate that they are temperature dependent. Parameter b exhibits Arrheneous-type temperature dependency with an activation energy of 36.84 kJ mol^{-1}, while parameter a decreases with increased temperature and at lower temperature does not vary significantly. Dependency of these para-

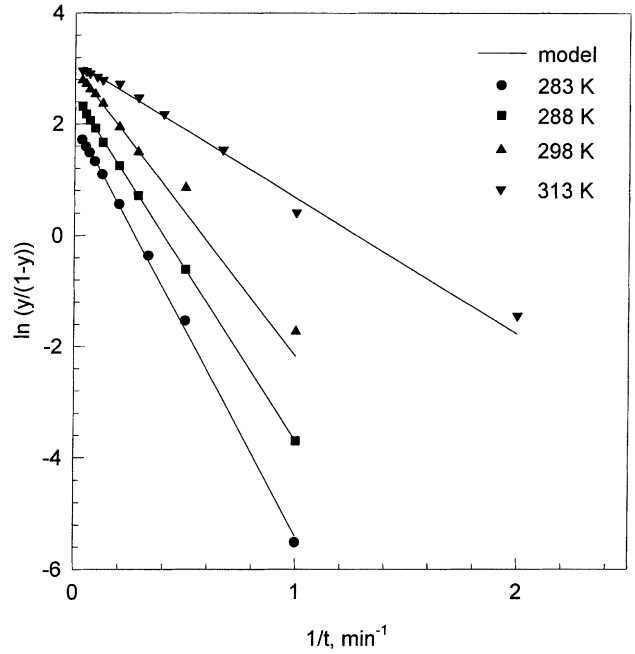

Fig. 4. Kinetic plots [ln(y/(1−y)) vs. 1/t] for leaching at different temperatures for D_p=95 μm.

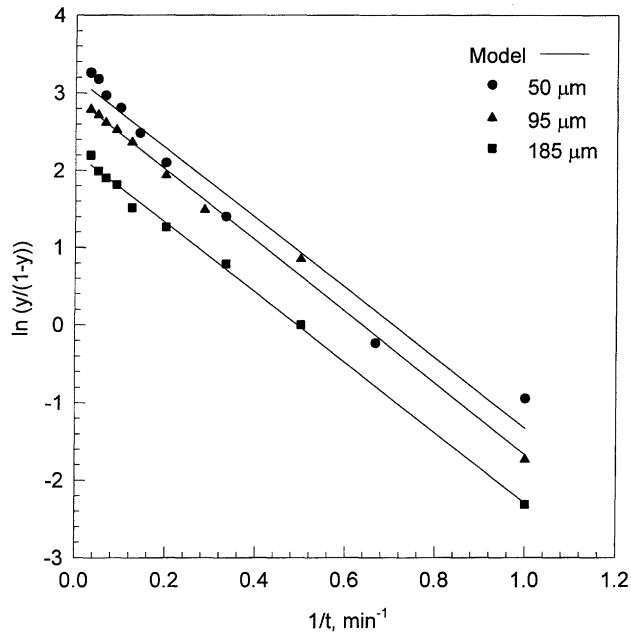

Fig. 5. Kinetic plots [ln(y/(1−y)) vs. 1/t] for leaching for different particle size at 298 K.

Table 2
Rate parameters (a and b) and initial rate at different temperatures and particle size

Temperature (K)	Rate parameters		Initial rate (min^{-1})	Half-life periods (min)	
	a (min)	b (min^{-1})		Experimental	Estimated
283	7.262	0.274	0.253	3.7	3.8
288	6.204	0.364	0.351	2.7	2.8
298	5.508	0.618	0.552	1.6	1.7
313	3.057	1.421	1.262	0.7	0.8

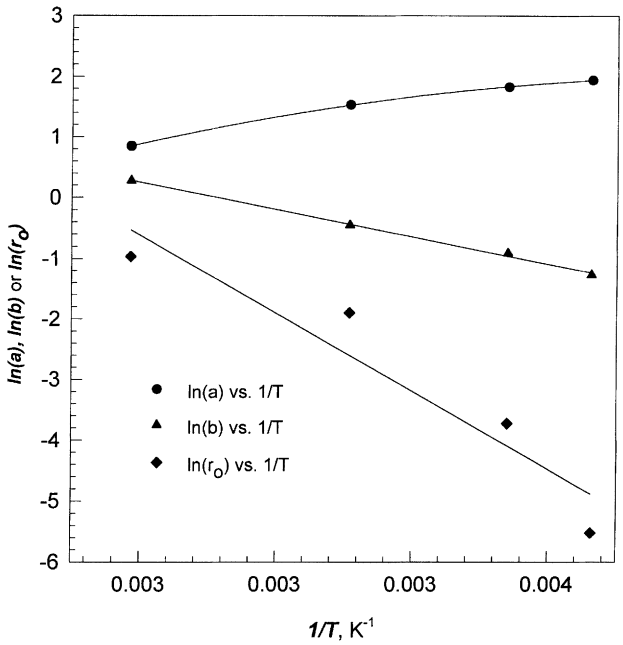

Fig. 6. Temperature dependence of parameters a, b and initial rate (r_0).

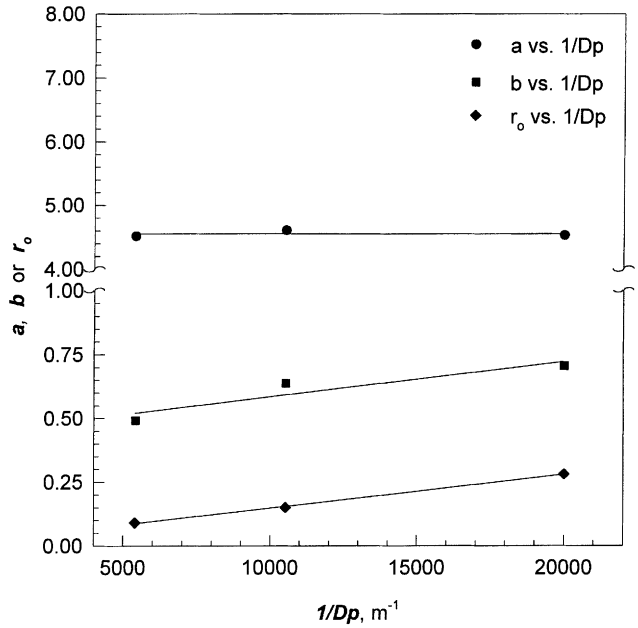

Fig. 7. Dependence of parameters a, b and initial rate (r_0) on particle size.

meters on external surface area is shown by plotting against $1/D_p$ in Fig. 7. Parameter b increases with $1/D_p$, while parameter a is almost constant. Initial rates (r_0) were estimated by graphical differentiation of leaching curves at zero time. In Fig. 6, $\ln(r_0)$ is plotted against $1/T$.

Independence of parameter a on external surface area of particles suggests that it represents mainly physical processes of crack development and pore plugging. Decrease in its value at higher temperature may be due to faster recrystallization and subsequent pore plugging. However, strong dependency of parameter b on temperature and initial external surface area, suggests that parameter b represents chemical rate processes. But the value of the activation energy is much lower than that of the initial rate. The difference may be due to higher solubilities of Al and ξ-phases which are present in the incipient leaching only.

5. Conclusion

Experimental leaching data of Raney-Ag alloy of different particle sizes at different temperature were obtained. The data fit well into Prout–Tompkins equation with rate constant, which is inversely proportional to the square of the time. The leaching process depends on two parameters, namely; a and b which appear to represent physical and chemical rate processes, respectively.

6. Nomenclature

a	rate parameter (min)
b	rate parameter (min^{-1})
c	integration constant
D_p	average particle diameter (μm)
k	time dependent rate constant (min^{-1})
r_0	initial rate of leaching (min^{-1})
T	absolute temperature (K)
t	time (min)
$t_{1/2}$	half-life period of the leaching process
y	fractional leaching as defined by Eq. (1)

Acknowledgements

Acknowledgment is due to King Fahd University of Petroleum and Minerals for use of their facilities.

References

[1] E. Justi, A. Winsel, Kalte Verbrennung – Fuel Cells, Franz Steiner Verlag, Weisbaden, 1962.
[2] H. Binder, A. Kohling, G. Sandstade, in: G. Sandstade (Ed.), From Electrocatalysis to Fuel Cells, University of Washington Press, Seattle, 1972.
[3] J. Yasumura, Kagaku Kyoiki 6 (1952) 733–740.
[4] S.K. Chaudhari, Ph.D. Dissertation, University of Poona, Pune, India, 1983.
[5] V.R. Choudhary, S.K. Chaudhari, A.N. Gokarn, Ind. Eng. Chem. Res. 28 (1989) 33–37.
[6] G. Baldi, R. Conti, E. Alaria, Chim. Eng. Sci. 33 (1978) 21–25.
[7] ASTM, E 738-80 (1985).
[8] O. Levenspiel, Chemical Rection Engineering, Wiley, New York, 1962.
[9] W.G. Moffatt, The Handbook of Binary Phase Diagrams, General Electric, Schenectady, 1981.
[10] E.G. Prout, F.C. Tompkins, Trans. Faraday Soc. 40 (1940) 488–498.
[11] S.J. Gregg, R.K. Pracker, R.H. Wheatley, J. Chem. Soc. (1955) 46–55.